

# Experimental Study of Different Electrokinetic Configurations for Desalination of a Brick Wall



Jorge Feijoo, Mónica Alvarez de Buergo, Rafael Fort, and Nevin Aly

**Abstract** Salt weathering is recognized as one of the main deterioration mechanisms that affect cultural heritage. The damage caused by this decay mechanism can range from simple aesthetic damage, when salts crystallize on the surface as efflorescence, to cause the loss of material, when salts crystallize beneath the material surface as sub- and crypto-efflorescence. To reduce the risk associated with salt-induced deterioration, the use of electrokinetic treatments, as desalination applied on-site, is undoubtedly the one that has allowed obtaining high extraction percentages in a short period of time. This study evaluates the efficacy of a new double electrode system at the anode (DA setup), to overcome the results achieved with the traditional electrokinetic configuration, using only one electrode (SA setup), to desalinate a brick masonry wall, located in the ancient stables of the eighteenth century Bernstorff Palace (Gentofte-Denmark), which is affected by salt-induced decay. The obtained results show that the DA setup allows maintaining higher moisture content in poultices located at the anode than using SA setup. This fact allows a proper and lasting current flow, which enhances the removal efficacy of all the anions present in the wall.

**Keywords** Salt-induced decay · Brick wall · Nitrates · Sulfates · Electrokinetic technique · Desalination · Double anode system · Anodic configuration

---

J. Feijoo · M. A. de Buergo · R. Fort  
Institute of Geosciences - IGEO (CSIC-UCM), C/Doctor Severo Ochoa, 7, 28040 Madrid, Spain  
e-mail: [j.feijoo@csic.es](mailto:j.feijoo@csic.es); [jfeijoo@tud.uvigo.es](mailto:jfeijoo@tud.uvigo.es)

J. Feijoo  
Defense University Centre, Spanish Naval Academy, Plaza de España S/N, 36920 Marín, Spain

N. Aly (✉)  
Faculty of Petroleum and Mining Engineering, Department of Science and Engineering  
Mathematics, Suez University, Suez 43512, Egypt  
e-mail: [nevin.aly@suezuniv.edu.eg](mailto:nevin.aly@suezuniv.edu.eg)

## 1 Introduction

Salt weathering is considered as one of the most widespread decay mechanisms that affect porous materials used in building constructions (ornamental rocks, mortars, bricks...). The damage caused by this agent can cause material loss at the surface, which in the case of cultural heritage can be considered as an historical and artistic damage of inestimable value (Aly and Hamed 2020; Rovella et al. 2020). For this reason, there are numerous studies focused on: (1) modelling the physical damage caused by salts, i.e. crystallization pressure (Rossi-Manaresi and Tucci 1991; Scherer 2004), hydration pressure (Flatt 2002; Tsui et al. 2003) and the pressure caused by the different coefficients of thermal expansion between the porous material and salt (Cooke and Smalley 1968; Lubelli et al. 2004), (2) analysing environmental conditions that affect crystallization-dissolution and hydration cycles of each salt (Arnold 1981; Charola 2000; Charola et al. 2006; Aly et al. 2015), and (3) developing and optimizing treatments, both for desalination by poultices (Vergès-Belmin and Siedel 2005; Lubelli and van Hees 2010; Pel et al. 2010), immersion baths (Unruh 2007), sacrificial mortars (Feijoo et al. 2021; Ergenç et al. 2020; Husillos-Rodríguez et al. 2018), surfactants (Lubelli et al. 2010; Gupta et al. 2012; Rivas et al. 2017), electrochemical techniques (Ottosen and Rørig-Dalgaard 2009; Feijoo et al. 2015, 2017a), or to reduce the accessible porosity by the application of consolidation treatments (de Rosario et al. 2017; Feijoo et al. 2017b, 2020a), in order to diminish the damage caused by this agent.

The main strategy currently used to reduce the damage caused by salts is focused on decreasing the content of salts present in the material (i.e. desalination techniques). The electrokinetic technique is always shows a great efficiency, in terms of salt content removed versus time both at laboratory scale and in pilot tests (Ottosen and Christensen 2012; Feijoo et al. 2013, 2017d). The higher desalination rate achieved by this technique is due to (1) the faster migration speed experienced by ions under the presence of an electric field (as stated in Paz-García et al. (2013), for a monovalent ion and at 298 °K, the ionic mobility is approximately 40 times higher per applied volt than the diffusion coefficient of the same anion), (2) the lesser influence exerted by the material's pore structure when the ions must be mobilized to the outside, which allow achieving similar extraction percentages regardless of the material to be treated (Feijoo et al. 2015) and (3) the higher penetration depth of the treatment. By means of electrokinetic techniques, it is possible to force the mobilization of all those ions that are found in areas of the material through which the electric field will circulate. Therefore, this technique allows to overcome the depth limitations that others have, such as the application of poultices, which hardly desalinate above 4 cm in depth (Rivas et al. 2017, Sawdy-Heritage et al. 2008).

The physical principle by which electrokinetic techniques function is relatively simple: when an electric DC field is applied, through a porous material with high ion content, the ions transport the current and are forced to migrate towards the electrode of opposite polarity. Consequently, there is a decrease in the ionic content in the material (which is reflected by an increase in the electrical resistance that opposes

against the current flow), and an increase in the ionic content in the vicinity of the electrodes. During this process, some mechanisms take place: (1) the electrolysis of water at the surface of the electrodes, which causes that extreme pH values are reached in these areas, and (2) movement of water towards one of the electrodes, depending on the surface charge of the porous material. In most porous materials this movement of water (by electro-osmosis) occurs from the anode towards the cathode, causing a differential drying rate between the materials located at each electrode (Ottosen et al. 2008; Bertolini et al. 2009; Franzoni 2014). This fact has an influence on the proper current flow between anodes and cathodes due to the loss of water that hinders the contact between the electrode and the poultice, and also reduces the amount of free ions that can transport the current.

In order to improve the operation of the technique, an electrokinetic casing that works with two electrodes connected in series, within the same compartment, has recently been developed at laboratory scale (Feijoo et al. 2018). This new approach allows modulating the net amount of  $H^+$  ions generated on the surface of the electrode closest to the porous material to be treated, in order to (1) maintain the pH at the desired value, and (2) humidify the materials located inside the casing, which are used to retain the ions removed and improve the contact between the electrode and the material to be treated. This humidifying process guarantees the correct transport of the current for longer.

The present paper assess the desalination results achieved from a pilot test plant made on a brick wall, comparing the results achieved using electrokinetic casings with a double electrode system at the anodes with those achieved with only one electrode.

## 2 Material and Methods

### 2.1 Description of the Building

The locality selected for the test plant was the stable of the Bernstorff Palace built in the middle of the eighteenth century. This stable, built with Danish bricks bonded with lime mortar and coated with plaster, is situated in Gentofte, municipality located at 9 km from Copenhagen (Denmark).

The desalination test was performed on the inner face of the west wall (Fig. 1a), which showed an advanced state of alteration caused by salts: efflorescence, granular disintegration of the mortar, scaling and roundness of the brick's corners, among other factors. External facade is partially covered with cement layer, as part of a previous desalination process (Fig. 1b). However, this cement layer has not been removed so it is possible that it is currently acting as a source of salts.

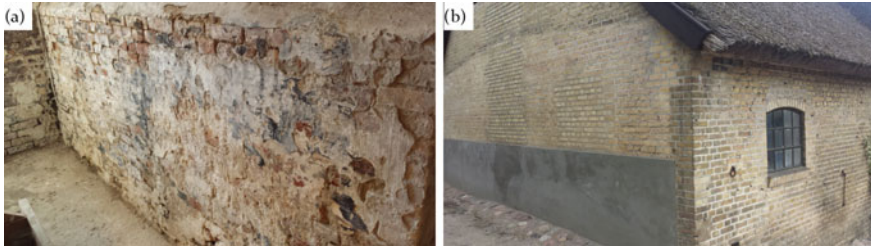


**Fig. 1** Brick wall on which the pilot test was made (inner part: **a**, outer part: **b**)

## 2.2 *Electrokinetic Desalination Setup*

The test was carried out from 02.06.2014 to 07.08.2014 (i.e. 66 days). For this pilot test, 12 electrokinetic casings (6 anodes and 6 cathodes) were used, which were distributed following a staggered distribution along the wall in two rows (Fig. 2).

The electrokinetic casings used in this study (50 cm long) are similar to those used in previous interventions (Ottosen et al. 2012) but with some necessary modifications, in order to allow them hosting one or two electrodes depending on the case (Feijoo et al. 2017c). The configuration with two electrodes at the anode connected in series is named double-anode (DA) and with only one electrode single-anode (SA).

Each casing is composed of two main pieces (Fig. 3): (1) A plastic frame whose mission is similar to the electrokinetic reactors used in the laboratory, i.e. to house all the materials necessary to carry out the desalination treatment, such as electrodes (in this case inert titanium-MMO mesh electrodes) and poultices, and (2) a movable plastic bottom located inside the plastic frame but behind all the previous elements. This piece must provide the necessary pressure, as the treatment progresses and the poultices lose volume, through the drying process, in order to guarantee the contact between the poultice and the wall.

The poultices used were (Fig. 3): At the cathode a poultice made of kaolin with a water content of 37.9% (named as P-C). At the anode, two different poultices were used in the DA configuration, the furthest was a poultice made of cellulose with a water content of 83% approximately (named as P-A1), while the closest made of calcium carbonate: kaolin in a weight ratio 2:1 with a water content of 30%. In the SA configuration, the casing was filled only with the poultice P-A2.

The electric field established between the electrodes E1 and E2, allows regulating the net amount of  $H^+$  generated at each electrode surface, as shown in the following equations that model the behavior of the DA configuration:

$$\text{At electrode E1 : } \Delta[H^+] = Q_1/Fw = I_1 t/Fw \quad (1)$$

$$\text{At electrode E2 : } \Delta[H^+] = Q_2/Fw = (I_2 - I_1) t/Fw \quad (2)$$

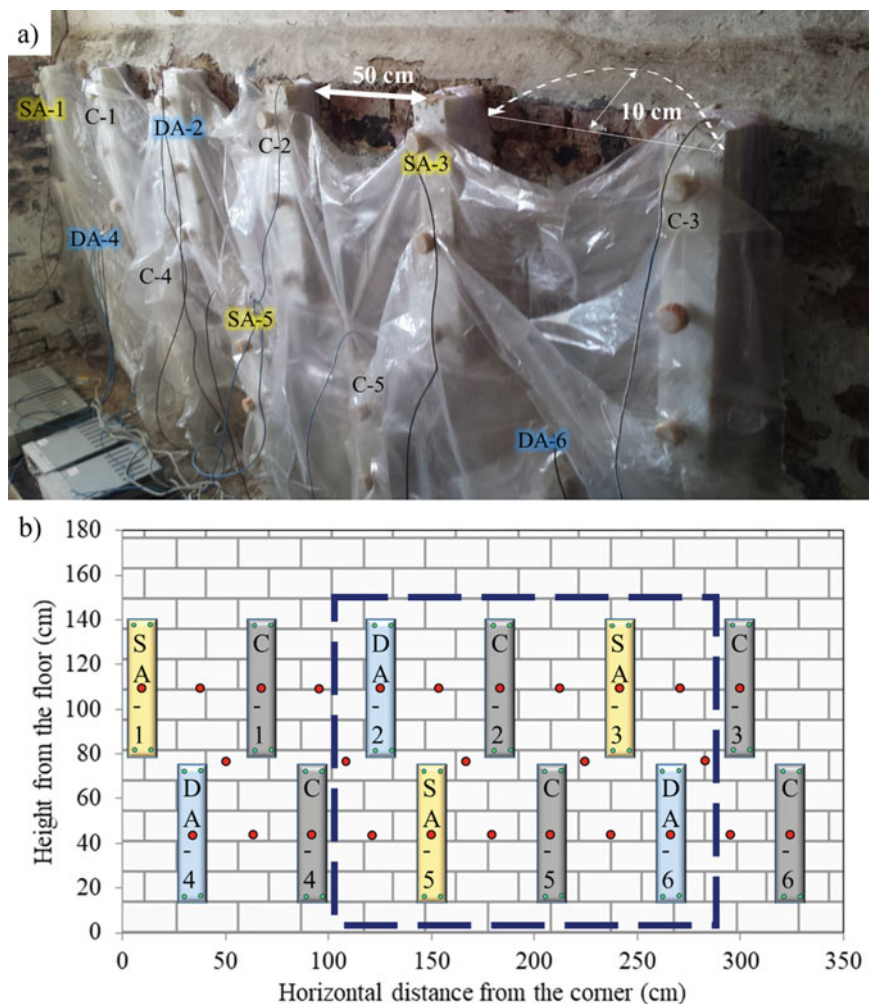
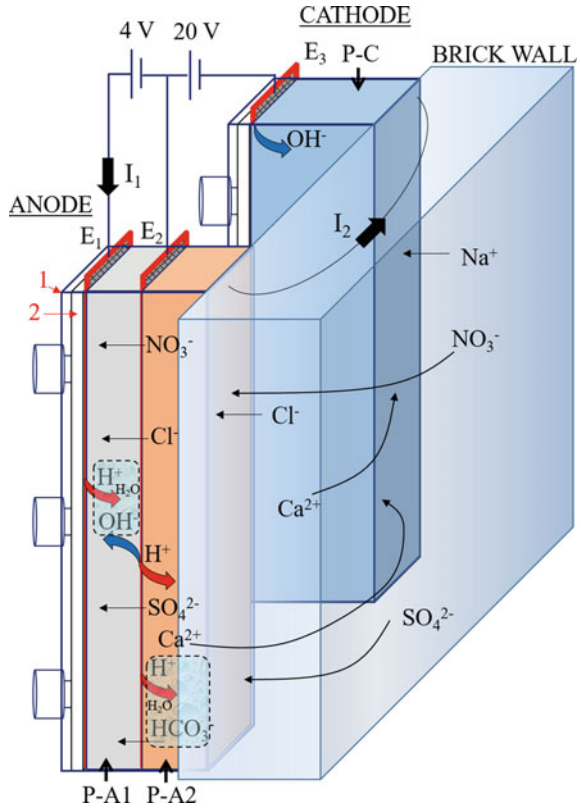


**Fig. 2.** **a** Photograph of the pilot test conducted on the west wall of the stable, showing the staggered distribution of the electrokinetic casings, the distance between them and the maximum expected depth of electric field penetration, and **b** Scheme with the distribution of the casings and sampling points made on the brick wall before (green circles made in the 4 corners of each casing to fasten it to the wall with screws), and after (red circles) the treatment. Also, the area used to compare the effectiveness of each type of anode is highlighted with a blue box in dashed line.

where  $Q$  is the circulating charge in C;  $F$  the Faraday's constant (96,485 C/mol),  $w$  the volume of the compartment,  $I$  the circulating current in A and  $t$  the time elapsed in s.

Therefore it is possible to regulate the amount of  $H^+$  and  $OH^-$  ions generated on the electrode E2 surface to buffer the pH to the desired value and generate water.

**Fig. 3** Diagram of one anodic casing, with the double anode configuration (electrodes E1 and E2), and one cathodic casing where the electrode E3 is hosted. Also, the different poultices used in each compartment (Anode: P-A1 and P-A2; cathode: P-C) and the two main parts that make up each casing (the plastic frame (1) and the movable plastic bottom (2)) are shown



For example,  $[H^+] = [OH^-] \rightarrow pH = 7$  if  $I_1 = I_2$ .

Once the electrokinetic casings were fastened and the titanium electrodes were connected to the respective power supplies (2 power supplies for the DA configuration and only 1 for the SA one), a constant voltage of 20 V was applied between electrodes E2 and E3, and in the case of DA configuration a constant voltage of 4 V was applied between electrodes E1 and E2. In order to ensure that all the potentials supplied by the sources are correct, all cathodes were short-circuited and grounded.

In addition, an automatic irrigation system was installed to moisten the brick wall with water during the treatment. This system provided water through drippers for 20 min every 3 h.

### 2.3 Desalination Treatment Monitoring and Effectiveness

Before carrying out the treatment, the plaster coating was removed and the entire wall was brushed. After that, and in order to identify the main anions present in the brick wall, forty-eight powder samples were collected, during the mounting of the electrode casings, by drilling (from the surface up to 10 cm in depth) in each of its four corners. The samples were dried, weighed and stirred in 25 mL of ultrapure water during 4 h. After filtration, the anion content was quantified with ion-chromatography (IC), using an IC Dionex ICS-1100. With these data, a mapping of each anion was performed using kriging as a statistical interpolation method. In order to know whether the anion content can involve a risk for the masonry wall or not, the only accessible threshold values established by the Austrian standard ÖNORM B 3355-1 (2006) was used. This standard establishes, specifically for brick masonries in general, three categories depending on the concentration of each anion. Concentrations above the upper limit involve a risk for the material and for this reason, it is necessary to carry out an active desalination intervention. Below the lower limit, no damage is expected, and between both limits, it is advisable to carry out a specific study. For the main anions, these limits are:  $\text{Cl}^-$  (0.10–0.03 wt.%),  $\text{NO}_3^-$  (0.15–0.05 wt.%), and  $\text{SO}_4^{2-}$  (0.25–0.10 wt.%).

During the treatment, measurements of intensity and resistivity between the electrodes connected to the same power supply were taken using a digital multimeter. The evolution of these parameters gives an idea about the progress of the treatment. Their subsequent analysis, along with other parameters, can indicate whether the increase in resistance is caused by a decrease in the ion content or by a loss of water in any of the materials used (i.e. poultrices or brick wall). In addition, the loss of water in the poultrices was analyzed indirectly by inserting, from the upper part of each electrokinetic casing, a plastic rod inside each poultrice to assess their resistance against penetration.

At the end of the treatment, three samples per poultrice were taken from each casing at different heights (from top to bottom). Each sample was used to measure the water content (following the gravimetric method), conductivity (adjusting the conductivity values following the expression proposed by Unruh (2007)), pH, and the anion content by IC (following the same procedure commented above).

Finally, in order to quantify the anion content that remains in the brick wall, a new in-depth sampling was carried out once the wall was already dry. Drilling powder samples were collected in different areas: on every area where each casing was placed, between casings, and between rows (Fig. 2b red circles). The efficacy of the desalination treatment was calculated comparing the ratio between the concentrations of each ion before and after the treatment, taking in both cases, as a data point, the concentration that exists just underneath the midpoint of each casing.

In all cases, to compare the results obtained with each anodic configuration, this study compares those casings that have similar boundary conditions, in terms of the row in which is placed (i.e. similar height) and the number of casings that surrounds it. For this reason, the following anodic casings are compared: SA-3 versus DA-2 and SA-5 versus DA-6.

### 3 Results and Discussion

#### 3.1 Anion Content Before the Treatment

The anion content measured in the drilling samples taken from the corners of each electrokinetic casing (Fig. 2b, green dots) showed that the main anions present in the brick wall were sulfates (with an average value around 5.52 wt.% along the entire wall) and nitrates (1.46 wt.% on average) respectively. In both cases the average concentration of both anions exceeded the upper limit established by the Austrian standard ÖNORM, which justifies that an active salt removal is necessary.

The distribution of both anions in height showed that the highest concentration of nitrates was achieved above 1 m high (Table 1), especially in the area where the casings SA-3 and C-3 were located (with concentration values ranging from 2.47 to 7.79 wt.%). In the case of sulfates, the highest concentrations were achieved 1 m high from the ground, with an average value around 7.37 wt.%.

The presence of both ions, as stated in (Arnold 1981; Grossi and Esbert 1994; Charola 2000; Gómez-Heras et al. 2004), seems to be related to (1) leaching processes of some construction materials such as the plaster coating, (2) residues of animal droppings and (3) the capillary rise of groundwater from areas where fertilizers are usually used.

**Table 1** Average of nitrate, sulfate and chloride content (in wt.%) analysed in the brick wall samples taken underneath the corners of each electrokinetic casing (initial content) and just underneath the midpoint of each casing (final content). Also, the efficacy achieved after the desalination treatment is shown

Row	Anode	Nitrate			Sulfate			Chloride		
		Before	After	Efficacy	Before	After	Efficacy	Before	After	Efficacy
Upper	SA-1	2.348	0.372	84.16	6.080	0.999	83.57	0.031	0.002	93.55
	DA-2	1.247	0.023	98.16	6.056	1.028	83.03	0.019	0.014	26.30
	SA-3	2.467	0.057	97.69	7.197	0.837	88.37	0.022	0.003	86.36
Lower	DA-4	0.049	0.013	73.47	0.507	0.222	56.21	0.013	0.002	84.62
	SA-5	0.112	0.003	97.32	1.217	0.068	94.41	0.004	0.011	-175.00
	DA-6	0.315	0.088	72.06	1.987	0.036	98.19	0.007	0.014	-100.00
	Cathode	Before	After	Efficacy	Before	After	Efficacy	Before	After	Efficacy
Upper	C-1	0.776	0.073	90.59	12.862	0.388	96.98	0.014	0.010	28.57
	C-2	1.688	0.020	98.82	9.516	0.281	97.05	0.014	0.015	-7.14
	C-3	7.785	0.095	98.78	2.503	0.604	75.87	0.110	0.016	85.45
Lower	C-4	0.025	0.004	84.00	0.104	0.055	47.12	0.006	0.012	80.00
	C-5	0.177	0.000	100.00	0.708	0.047	93.36	0.006	0.009	-50.00
	C-6	0.574	0.109	81.01	17.465	1.194	93.16	0.009	0.003	66.67



As shown in Table 1, the presence of chloride was very low, being in practically all cases below the risk level established by the Austrian standard.

### 3.2 Resistivity Measurements

The evolution of the resistivity showed a similar trend (Fig. 4): low and similar values at the beginning that increase during treatment. However, as the treatment progresses, there was a distancing between the resistivity measurements recorded in the casings with SA and DAS configuration. From day 20 approximately, the resistivity values reached in casings with SA configuration were much higher than those with DAS configuration, regardless of the row in which they were located. This different behavior was related to the different drying rate that occurs in the poultices located in the different type of anodic configurations. While in the SA configuration the anode poultice dried fast, hindering, in consequence, the current flow, with the DA configuration this drying process was slowed down by the generation inside the casing of water molecules. This fact was corroborated by inserting plastic rods inside each electrokinetic casing to check the degree of humidity of each poultice. The poultices hosted in the SA configuration hardened much earlier than those hosted in the DA configuration.

Summarizing, in the DA casings the values of current intensity were greater for longer than those reached in the SA casings, in virtually the entire pilot test. However, on day 66, the difference between the intensity values was reduced (moment in which it was decided to stop the test).

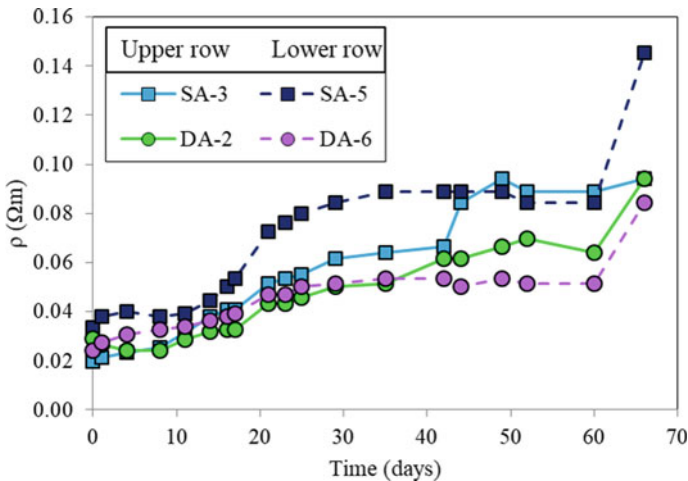


**Fig. 4** Resistivity measurements registered during the treatment in the anodes with the same boundary conditions (SA-3 vs DA-2 and SA-5 vs DA-6)

### 3.3 Analysis of the Poultices

#### 3.3.1 Water Content

The differences observed between the final water contents reached in the anodic P-A2 poultices, after 66 days of treatment, were very low between both configurations (around 21% of water in both cases). However, this does not mean that during the previous days the water content present in the DA configuration was not higher than that reached in this poultice hosted in the SA configuration. As indicated above, the periodic checks made by inserting a plastic rod clearly showed that the poultice P-A2 hosted in the SA configuration dried faster than that hosted in the DA configuration. Therefore, this result only indicates that at the end of the treatment, the differences in the water content between P-A2 poultices were reduced. The application of constant voltage, instead of constant current, in the power supplies did not allow to generate enough net amount of OH<sup>-</sup> ions in the vicinity of the electrode E2 to maintain the degree of humidity inside this P-A2 poultice for a longer time. For this reason, on day 66 the intensity values were similar for all the electrokinetic casings.

Regarding the poultices P-A1 used in the DA configuration, although they have lost about 50% of their initial water content, they still maintain a sufficient water content (approximately 40 wt.%) for maintaining an electric field between the electrodes E1 and E2.

Finally, with respect to the cathodic poultices (P-C), the weight loss was much lower than that registered by the anodic poultices (these poultices only loss around 15% of the initial water content). This result could be related to the establishment of an electroosmotic process which has slowed down this drying process.

#### 3.3.2 pH and Conductivity

At the end of the treatment, the pH values reached by each poultice were different depending on the electrode that they hosted (Table 2). In the anode poultice P-A2, that hosted the electrode E2, the pH values were similar regardless of the type of anode (around 7). This fact indicates that the pH buffering system of both configurations worked perfectly, as occurs in previous studies (Ottosen et al. 2012; Feijoo et al. 2017a, 2018), preventing the brick wall to be exposed to acidic pH values that can cause chemical alteration processes.

In the anode poultice P-A1 (used in the DA configuration), in which the electrode E1 is hosted, acidic pH values around 3 were reached. This fact is related to the proper operation of the double electrode system since in this configuration the true anode of the system is the electrode E1. This electrode is hosted in a medium that has a zero buffering capacity of the pH (i.e. cellulose), favoring in consequence the acidification of the medium around the electrode, due to the generation of H<sup>+</sup> groups at the electrode surface; it also favors the generation of OH<sup>-</sup> groups on the surface of the electrode E2 that is in the front. The migration of the H<sup>+</sup> groups, from the

**Table 2** pH and adjusted conductivity values (Kad, in  $\mu\text{S} \cdot \text{L/g} \cdot \text{cm}$ ) for each poultice used to fill each casing

Anode	pH		Kad	
	P-A1	P-A2	P-A1	P-A2
SA-1	–	7.05	–	0.027
DA-2	4.10	7.30	0.068	0.043
SA-3	–	7.54	–	0.027
DA-4	1.76	7.46	0.107	0.007
SA-5	–	7.49	–	0.012
DA-6	3.15	7.26	0.072	0.036
Cathode	pH		Kad	
	P-C		P-C	
C-1	11.34		0.019	
C-2	11.30		0.012	
C-3	11.51		0.014	
C-4	11.47		0.010	
C-5	11.36		0.009	
C-6	11.40		0.015	

electrode E1 towards the vicinity of the electrode E2, favors the generation of water molecules.

In all the cathodic casings, the pH values were similar and high (around 11.30). These high pH values show that in future on-site applications a solution similar to that used in the anode with a double electrode configuration could be applied to buffer the pH reached in the closest areas to the material to be treated, as has been demonstrated at laboratory scale in Feijoo et al. (2020b).

Regarding conductivity, the highest values were reached with the DA configuration, especially in the poultice P-A1. This result is indicative of: (1) the ionic content in the poultices hosted in the DA casings was higher than in the other casings. This result could be related to the greater intensity that flowed in these anodes. (2) A large part of the anions that were initially retained by the poultice P-A2 was subsequently forced to migrate to the poultice P-A1. This fact favors that the storage capacity of the poultice P-A2, which is smaller by the pore size of the kaolinite than that of the poultice P-A1 made of cellulose (Bourgès and Vergès-Belmin 2008; Pel et al. 2010), is maintained for a longer time.

Using the SA configuration, the conductivity values were similar and higher to those obtained in the cathodes, with the exception of those achieved with the SA-5 casing, where the value was similar to those reached at the cathodic casings. The lower conductivity achieved in the poultices hosted in the SA casings is related to the lower current flow, caused in large part by the faster loss of water, which made it difficult to mobilize a greater quantity of anions within the SA casings.

### 3.3.3 Anion Content

The chromatography results showed that in general: (1) nitrate has been removed to a greater extent than sulfate. This is due to the greater mobility of nitrate, which causes that the current was transported to a greater extent by this anion, similar result to that achieved in previous studies (Feijoo et al. 2017a). (2) The amount of each anion retained inside the casings was higher for those casings located in the upper row than for those located in the lower row. This fact is related to the initial distribution of salts in height (Fig. 5 and Table 1).

Regarding the two anode configurations assessed in this study, for anodes that had the same boundary conditions, the configuration that allowed extracting a greater amount of nitrate and sulfate was the DA configuration (Fig. 5), which agrees with the conductivity measurements discussed above.

This different behavior is clearly related to the double anode configuration and with the ability that this system provides to keep the poultices moist for longer. For the same ionic content in the medium, the higher the humidity, the higher the intensity value that circulates through the material, and the greater the amount of ions mobilized inside the casings (it must be taken into account that the ions are the responsible for the transport of the current).

At the cathode casings, the nitrate content was in general very low (between 0.007 and 0.04 wt.%), being in this case the sulfate the main anion retained by the P-C poultices. In both cases the extraction is caused by the typical process associated to desalination with poultices: advection and diffusion processes (Pel et al. 2010).

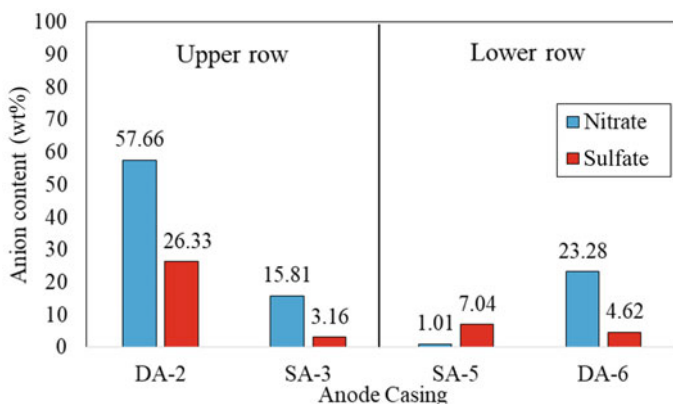


**Fig. 5** Concentrations of  $\text{NO}_3^-$  (blue) and  $\text{SO}_4^{2-}$  (red) retained in the poultices that fill the anodes with the same boundary conditions (DA-2 vs SA-3 and SA-5 vs DA-6)

### 3.4 Analysis of the Brick Wall. Final Ion Content

At the end of the treatment, the anion content present in the entire wall was considerably reduced, reaching efficacy percentages in most cases that exceeded 80%, even 90% (Table 1). These percentages allow classifying this technique as a treatment of high or very high efficacy, according to the classification established by a desalination European project (Desalination Project E 2006).

In general, the highest efficiency percentages were reached in those wall areas where the cathodic casings were located. This is due to the fact that the anions, under the DC field, are forced to migrate from these areas towards those closest to the anodes, where their extraction takes place.

With respect to the two anodic configurations, and comparing those casings with similar boundary conditions, it is appreciated that although in almost all cases the greatest reductions were achieved with the DA configuration, these results cannot be considered as data to establish what the best configuration is. This is because the distribution of salts is not homogeneous along the brick wall. For example, in the particular case of nitrate, the efficiency percentages were higher in the upper part of the wall than in the lower part, although the final contents were lower in the lower part of the wall. This is related to the initial distribution of this anion, which was higher above 1 m high. In the case of sulfate, the differences between rows were smaller due to the fact that its initial distribution was more or less homogeneous up to 1 m high.

In spite of the high reductions achieved, there is still in the brick wall some areas with anion concentrations that exceed the upper limit value established by the Austrian standard ÖNORM (0.15 wt.% for nitrate and 0.25 wt.% for sulfate): in the case of nitrate, it would be the area surrounding the SA-1 casing, while in the case of sulfate, it would be the entire upper area of the wall and the lower area located in the vicinity of the C-6 casing. Therefore, it would be advisable that in the future a second intervention of the wall would be carried out again to remove completely the anions presents.

## 4 Conclusions

From the obtained results, the following conclusions can be established:

- The use of the electrokinetic treatment allows reaching high efficiency percentages of reducing salt content (nitrate and sulfate) throughout the entire wall (higher than 80% in both cases), removing after the treatment around 206 g nitrate and 106 g sulfate.
- The resistivity measurements registered during the treatment, together with the analysis of the ionic content retained in the poultices and the resistance that these oppose to the penetration of a plastic rod, showed that the use of two electrodes at the anode (DA configuration) improves the wetting process of the anodic poultice

P-A2, which is in contact with the brick wall. This fact improves the current flow between the DA casings with those casings of different polarities that surround it (i.e. cathodes). In consequence, with this DA configuration, more ions can be mobilized from the wall towards the poultrices.

- The use of the DA configuration allows buffering the pH by means of the electric field established between the electrodes located in the anode. This fact allows reducing the amount of the poultice made of calcium carbonate: kaolin and introducing in the casing a poultice made of cellulose, which increases the ion storage capacity of the casing.

**Acknowledgements** This research was funded by the TOP Heritage program (P2018/NMT-4372) of the Community of Madrid. J. Feijoo's work is supported by the Ministerio de Ciencia Innovación y Universidades, Spanish Government, through a Juan de la Cierva grant. Special acknowledgments to the professional support of the Interdisciplinary Thematic Platform from CSIC Open Heritage: Research and Society (PTI-PAIS) and an I-COOP 2018 cooperation project (COOPB20379) between the coauthors of this paper (Egypt and Spain), funded by CSIC.

## References

- Aly N, Hamed A (2020) The impact of salt crystallization on the building stones of AL-Azhar mosque from historic Cairo–Egypt. *Int J Conserv Sci* 11(4):895–904
- Aly N, Gomez-Heras M, Hamed A, Álvarez de Buergo M, Soliman F (2015) The influence of temperature in a capillary imbibition salt weathering simulation test on mokattam limestone. *Mater Construcc* 65(317):e044. <https://doi.org/10.3989/mc.2015.00514>
- Arnold A (1981) Nature and reactions of saline minerals in walls. In: *The conservation of stone, II: preprints of the contributions to the International Symposium, Bologna, 27–30 October 1981*. Part A, Deterioration. Part B, Treatment
- Bertolini L, Coppola L, Gastaldi M, Redaelli E (2009) Electroosmotic transport in porous construction materials and dehumidification of masonry. *Constr Build Mater*. <https://doi.org/10.1016/j.conbuildmat.2007.12.013>
- Bourgès A, Vergès-Belmin V (2008) Comparison and optimization of five desalination systems on the inner walls of Saint Philibert Church in Dijon, France. In: *Salt weathering on buildings and stone sculptures, 22–24 October 2008, The National Museum Copenhagen, Denmark*
- Charola AE, Pühringer J, Steiger M (2006) Gypsum: a review of its role in the deterioration of building materials. *Environ Geol* 52:339–352 <https://doi.org/10.1007/s00254-006-0566-9>
- Charola AE (2000) Salts in the deterioration of porous materials: an overview. *J Am Inst Conserv*. <https://doi.org/10.2307/3179977>
- Cooke RU, Smalley IJ (1968) Salt weathering in deserts. *Nature* 220:1226–1227
- de Rosario I, Rivas T, Buceta G et al (2017) Surfactant-synthesized consolidants applied to a granitic medieval necropolis in NW Spain. Laboratory and in situ effectiveness evaluation. *Int J Archit Herit* 11:1166–1176. <https://doi.org/10.1080/15583058.2017.1354097>
- Ergenç D, Feijoo J, Fort R, Alvarez de Buergo M (2020) Effects of potassium ferrocyanide used for desalination on lime composite performances in different curing regimes. *Constr Build Mater* 259:120409
- Desalination Project E (2006) Assessment of desalination mortars and poultrices for historic masonry

- Feijoo J, Ergenç D, Fort R et al (2021) Addition of ferrocyanide-based compounds to repairing joint lime mortars as a protective method for porous building materials against sodium chloride damage. *Mater Struct* 54(1):14
- Feijoo J, Fort R, Gomez-Villalba LS et al (2020a) Electroprecipitation of magnesium and calcium compounds for weathering protection of ornamental rocks. *Cryst Growth Des* 20(4):2337–2355
- Feijoo J, Rivas T, Nóvoa XR, Ottosen LM (2020b) New double electrode system for the electrochemical desalination of building stones. *Int J Archit Herit* 14(5):678–693
- Feijoo J, Nóvoa XR, Rivas T, Ottosen LM (2018) Enhancing the efficiency of electrochemical desalination of stones: a proton pump approach. *Mater Struct Constr* 51 <https://doi.org/10.1617/s11527-018-1224-x>, <https://doi.org/10.1080/15583058.2018.1561962>
- Feijoo J, Matyščík O, Ottosen LM et al (2017a) Electrokinetic desalination of protruded areas of stone avoiding the direct contact with electrodes. *Mater Struct* 50:82. <https://doi.org/10.1617/s11527-016-0946-x>
- Feijoo J, Ottosen LM, Nóvoa XR et al (2017b) An improved electrokinetic method to consolidate porous materials. *Mater Struct* 50:186. <https://doi.org/10.1617/s11527-017-1063-1>
- Feijoo J, Rivas T, Nóvoa XR et al (2017c) Electrokinetic method and device for extracting ions from a porous structure (ES2617971)
- Feijoo J, Rivas T, Nóvoa XR et al (2017d) In situ desalination of a granitic column by the electrokinetic method. *Int J Archit Herit* 12:1–12. <https://doi.org/10.1080/15583058.2017.1370509>
- Feijoo J, Ottosen LM, Pozo-Antonio JS (2015) Influence of the properties of granite and sandstone in the desalination process by electrokinetic technique. *Electrochim Acta* 181:280–287. <https://doi.org/10.1016/j.electacta.2015.06.006>
- Feijoo J, Nóvoa XR, Rivas T et al (2013) Granite desalination using electromigration. Influence of type of granite and saline contaminant. *J Cult Herit* 14:365–376. <https://doi.org/10.1016/j.culher.2012.09.004>
- Flatt RJ (2002) Salt damage in porous materials: how high supersaturations are generated. *J Cryst Growth*. [https://doi.org/10.1016/S0022-0248\(02\)01429-X](https://doi.org/10.1016/S0022-0248(02)01429-X)
- Franzoni E (2014) Rising damp removal from historical masonries: a still open challenge. *Constr Build Mater* 54:123–136
- Gómez-Heras M, Benavente D, Álvarez de Buergo M, Fort R (2004) Soluble salt minerals from pigeon droppings as potential contributors to the decay of stone based cultural heritage. *Eur J Mineral*. <https://doi.org/10.1127/0935-1221/2004/0016-0505>
- Grossi CM, Esbert RM (1994) Las sales solubles en el deterioro de rocas monumentales. Revisión bibliográfica. *Mater Construcción*. <https://doi.org/10.3989/mc.1994.v44.i235.579>
- Gupta S, Terheiden K, Pel L, Sawdy A (2012) Influence of ferrocyanide inhibitors on the transport and crystallization processes of sodium chloride in porous building materials. *Cryst Growth Des*. <https://doi.org/10.1021/cg3002288>
- Husillos-Rodríguez N, Carmona-Quiroga PM, Martínez-Ramírez S et al (2018) Sacrificial mortars for surface desalination. *Constr Build Mater*. <https://doi.org/10.1016/j.conbuildmat.2018.04.029>
- Lubelli B, Nijland TG, van Hees RPJ, Hacquebord A (2010) Effect of mixed in crystallization inhibitor on resistance of lime–cement mortar against NaCl crystallization. *Constr Build Mater* 24:2466–2472 <https://doi.org/10.1016/j.conbuildmat.2010.06.010>
- Lubelli B, van Hees RPJ (2010) Desalination of masonry structures: fine tuning of pore size distribution of poultices to substrate properties. *J Cult Herit* 11:10–18. <https://doi.org/10.1016/j.culher.2009.03.005>
- Lubelli B, Van Hees RPJ, Groot CJWP (2004) The role of sea salts in the occurrence of different damage mechanisms and decay patterns on brick masonry. In: *Construction and building materials ÖNOR.M.B. 3355-1 (2006) Trockenlegung von feuchtem Mauerwerk — Teil 1: Bauwerksdiagnose und Planungsgrundlagen Berlin*. ASI Austrian Standards Institute Österreichisches Normungsinstitut (Herausgeber) Deutschland, Bundesrepublik, Beuth Verlag. 1:3355

- Ottosen LM, Christensen IV (2012) Electrokinetic desalination of sandstones for NaCl removal—test of different clay poultices at the electrodes. *Electrochim Acta* 86:192–202. <https://doi.org/10.1016/j.electacta.2012.06.005>
- Ottosen LM, Christensen IV, Rørig-dalgaard I (2012) Electrochemical desalination of salt infected limestone masonry of a historic warehouse. *Struct Faults Repair, Edinburgh Proc*
- Ottosen LM, Christensen IV, Rorig-Dalgård I et al (2008) Utilization of electromigration in civil and environmental engineering—processes, transport rates and matrix changes. *J Environ Sci Health A Tox Hazard Subst Environ Eng* 43:795–809. <https://doi.org/10.1080/10934520801973949>
- Ottosen LM, Rørig-Dalgaard I (2009) Desalination of a brick by application of an electric DC field. *Mater Struct* 42:961–971. <https://doi.org/10.1617/s11527-008-9435-1>
- Paz-García JM, Johannesson B, Ottosen LM, Ribeiro AB, Rodríguez-Maroto JM (2013) Simulation-based analysis of the differences in the removal rate of chlorides nitrates and sulfates by electrokinetic desalination treatments. *Electrochim Acta* 89:436–444
- Pel L, Sawdy A, Voronina V (2010) Physical principles and efficiency of salt extraction by poulticing. *J Cult Herit* 11:59–67. <https://doi.org/10.1016/j.culher.2009.03.007>
- Rivas T, Feijoo J, de Rosario I, Taboada J (2017) Use of ferrocyanides on granite desalination by immersion and poultice-based methods. *Int J Archit Herit* 11:588–606. <https://doi.org/10.1080/15583058.2016.1277282>
- Rossi-Manaresi R, Tucci A (1991) Pore structure and the disruptive or cementing effect of salt crystallization in various types of stone. *Stud Conserv.* <https://doi.org/10.2307/1506452>
- Rovella N, Aly N, Comite V, Randazzo L, Fermo P, Barca D, Alvarez de Buergo M, La Russa M (2020) The environmental impact of air pollution on the built heritage of historic Cairo (Egypt). *Sci Total Environ.* <https://doi.org/10.1016/j.scitotenv.2020.142905>
- Sawdy-Heritage AM, Heritage A, Pel L (2008) A review of salt transport in porous media: assessment methods and salt reduction treatments. In: *Salt weathering on buildings and stone sculptures (SWBSS)*, 22–24 October 2008, Copenhagen, Denmark
- Scherer GW (2004) Stress from crystallization of salt. *Cem Concr Res* 34:1613–1624. <https://doi.org/10.1016/j.cemconres.2003.12.034>
- Tsui N, Flatt RJ, Scherer GW (2003) Crystallization damage by sodium sulfate. *J Cult Herit* [https://doi.org/10.1016/S1296-2074\(03\)00022-0](https://doi.org/10.1016/S1296-2074(03)00022-0)
- Unruh J (2007) A revised endpoint for ceramics desalination at the archaeological site of gordion, Turkey. *Stud Conserv.* <https://doi.org/10.2307/1506839>
- Vergès-Belmin V, Siedel H (2005) Desalination of masonries and monumental sculptures by poulticing: a review. *Restor Build Monum an Int J = Bauinstandsetz und Baudenkmalpfl eine Int Zeitschrift.* <https://doi.org/10.1515/rbm-2005-6000>